Chemical Engineering Journal 463 (2023) 142356

Contents lists available at ScienceDirect

Chemical Engineering Journal

journal homepage: www.elsevier.com/locate/cej

Development of a sensitive luminescent probe to uncover new BRD4 inhibitors in living cells

Ying-Qi Song [a,1], Ke-Jia Wu [a,1], Zhiming Zhang [b], Tzu-Ming Liu [b], Chung-Nga Ko [c], Wei-Guo Zhu [d], Dik-Lung Ma [c,*], Wanhe Wang [c,e,*], Chung-Hang Leung [a,f,*]

[a] State Key Laboratory of Quality Research in Chinese Medicine, Institute of Chinese Medical Sciences, University of Macau, Macao, China
[b] Institute of Translational Medicine, Faculty of Health Sciences & Ministry of Education Frontiers Science Center for Precision Oncology, University of Macau, Taipa, Macau, China
[c] Department of Chemistry, Hong Kong Baptist University, Hong Kong, China
[d] Department of Biochemistry and Molecular Biology, Shenzhen University School of Medicine, Shenzhen, China
[e] Institute of Medical Research, Northwestern Polytechnical University, 127 West Youyi Road, Xi'an, Shaanxi 710072, China
[f] Department of Biomedical Sciences, Faculty of Health Sciences, University of Macau, Macao, China

ARTICLE INFO

Keywords:
Luminescent
Drug screening
BRD4
Inhibitor
Probe
Azelastine

ABSTRACT

Bromodomain-containing protein 4 (BRD4) is a reader of acetylated histones that regulates the invasion, metastasis and proliferation of cancer. Inhibition of BRD4 activity is an emerging strategy for anticancer. In this study, an iridium based-luminescent probe for screening BRD4 inhibitors *in cellulo* was developed. The **K293** probe was designed by linking a BRD4 nuclear translocation inhibitor as a "binding unit" to an iridium complex as a luminescent "signal unit". **K293** selectively binds to BRD4 in living cancer cells. Candidate compounds compete with **K293** for BRD4, resulting in a decrease in luminescence signal. The long luminescence lifetime of **K293** allows its luminescence signal to be distinguished from interfering fluorescence using time-resolved techniques in order to improve sensitivity. Hence, even potential BRD4 inhibitors that are undetectable by conventional fluorescence methods can be identified. As a proof-of-concept, Azelastine, an FDA-approved histamine 1 (H_1) antagonist was identified to be a potential BRD4 inhibitor using the **K293** probe. Azelastine binds to BRD4 protein in the cytoplasm to prevent its translocation into the nucleus, and suppresses cancer cell growth and migration. The results demonstrated that the probe could be useful for the future drug repurposing.

1. Introduction

Bromodomain-containing protein 4 (BRD4) is a reader of acetylated histones [1]. In the nucleus, the protein binds to the transcriptional start sites of expressed genes and phosphorylates the RNA polymerase II C-terminal domain (CTD) to stimulate RNA polymerase II-dependent transcription [1,2]. BRD4 also plays a critical function in transcriptional elongation by recruiting the positive transcription elongation factor complex (P-TEFb) [2]. However, aberrant BRD4 activity has been associated with the development of cancer. A previous study showed that BRD4 enhances the transcriptional activities of oncogenic factors, such as androgen receptor (AR), E-26 transformation-specific transcription factor (ERG) and NF-κB [3,4]. The expression of BRD4 is also positively correlated with biomarkers of cancer stem cells and is critical for the metastasis and invasion of melanoma, one of the most lethal cutaneous cancers. Inhibition of BRD4 suppressed the progression of breast cancer, prostate cancer and colorectal cancer [5–9]. Hence, inhibition of BRD4 is an emerging anticancer strategy [1,10–12]. Interestingly, our group has previously reported the small molecule **K197** as a BRD4 inhibitor and repressor of NF-κB-driven triple-negative breast cancer cells [13].

Current methods for screening BRD4 inhibitors are generally based on fluorescent or nanomaterial probes [14,15]. Fluorescence technology offers high sensitivity and convenience, which is commonly used for high-throughput screening (HTS) of bioactive molecules [16]. Some studies have reported the identification of potential BRD4 inhibitors using fluorescence polarization (FP) and homogeneous time-resolved fluorescence (HTRF) techniques. However, these methods often

* Corresponding authors.
E-mail addresses: edmondma@hkbu.edu.hk (D.-L. Ma), whwang0206@nwpu.edu.cn (W. Wang), duncanleung@um.edu.mo (C.-H. Leung).
[1] These authors contributed equally to this work.

https://doi.org/10.1016/j.cej.2023.142356
Received 27 October 2022; Received in revised form 6 January 2023; Accepted 7 March 2023
Available online 11 March 2023

generate false positive or negative results due to the intrinsic fluorescence of certain compounds [17], or interference from background fluorescence in the cell [18,19]. Therefore, novelty cell-based screening platforms for BRD4 inhibitors are required.

Iridium complexes have been widely explored as luminescence bioimaging probes for drug screening due to their desirable photophysical properties, including large Stokes shift, long emission lifetime, and ease of modifications [20,21]. Iridium complexes modified with biomolecule-targeting molecules have attracted interest as a new type of theranostic probe to screen inhibitors [22]. Typically, a targetable molecule-conjugated iridium probe consists of a "binding unit" that selectively binds to biomolecules, a "signal unit" that reveals the target analyte by converting the binding event into a luminescent signal, and a "linker" region that connects the binding unit and the signal unit [23]. In a previous study, our group identified **K197** as a selective BRD4 inhibitor [13]. This compound displayed potent anticancer activity in NF-κB-active MDA-MB-231 cells via antagonizing the protein–protein interaction (PPI) between BRD4 and acetylated RelA [13]. Therefore, we envisaged that **K197** could act as a "binding unit" for targeting BRD4.

In this study, the luminescent probe **K293** was developed by conjugated **K197** to an iridium scaffold. The inherent high quantum yield and tunable emission of the iridium complex renders **K293** an attractive scaffold for the development of bioimaging probes for tracking BRD4. Moreover, cellular screening assays are essential to most modern drug development projects [24]. The advantage of our **K293**-based screening method compared to *in vitro* assays is that it also screens for compounds that can cross cellular membranes and interact with BRD4 in a cellular context. Thus, our **K293** probe-based offers a powerful method for the real-time imaging study of BRD4 levels in living cells.

Recently, some research reported BRD4 is synthesized in the cytoplasm and needs to be translocated into the nucleus to promote tumor metastasis and cell plasticity [24,25]. The **K293** probe binds to BRD4 in the cytoplasm, preventing it from entering the nucleus. However, if the candidate compounds compete with **K293** for BRD4, the luminescence of **K293** probe will decrease. Using the long emission lifetime of **K293** probe allows its luminescent signal to be readily distinguished from the background signal of the compounds by using time-resolved techniques, thereby improving the sensitivity of the assay and preventing false negative results. As a proof-of-concept, a cellular screening platform employing **K293** probe was used for screening BRD4 inhibitors from an FDA-approved drugs database, resulting in the identification of Azelastine as a potential BRD4 inhibitor with anticancer activity. We anticipate that this luminescent probe-based screening system could facilitate the development of more anti-BRD4 drugs by overcoming the intrinsic fluorescent interference of both bioactive compounds and the cell background (Scheme 1).

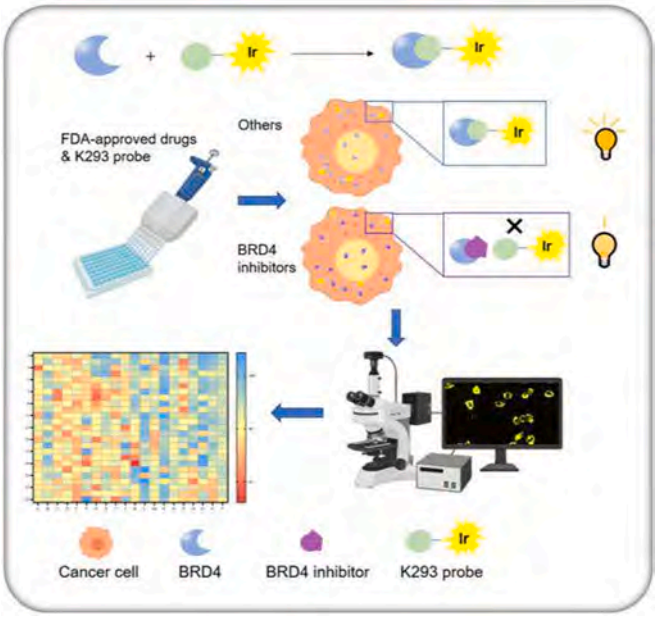

Scheme 1. A cellular screening platform for potential BRD4 inhibitors using the luminescent **K293** probe.

2. Experimental

2.1. Cellular thermal shift assay (CETSA)

Cellular thermal shift assay was performed to monitor the target engagement of Azelastine in A375 cell lysates. Briefly, cell lysates from 2×10^6 A375 cells were collected, diluted in PBS and separated into aliquots. Each aliquot was treated with Azelastine (10 μM) or DMSO after incubation at room temperature for 30 min. The compound-treated lysates were heated individually at different temperatures (45 to 70 °C). The heated lysates were centrifuged and the supernatants were analyzed by SDS-PAGE followed by immunoblotting analysis with the indicated antibody.

2.2. Confocal imaging

A375 cells were seeded into confocal dishes with glass-bottom. 12 h later, the cells were incubated with complex **K293** probe and Azelastine at the indicated concentrations for 2 h, followed by washing dishes with PBS for 3 times. Luminescence imaging was carried out using a Leica TCS SP8 confocal laser scanning microscope system at an excitation wavelength of 405 nm. The quantitation of mean luminescent intensity was calculated by ImageJ software.

2.3. Phosphorescence lifetime imaging (PLIM)

K293 (10 μM) or nitroxoline (10 μM) were added to A375 cells and the cells were incubated for 2 h. The cells were pre-fixed with 4% paraformaldehyde for 20 min and washed three times with phosphate-buffered saline (PBS), followed by imaging using a Nikon Eclipse Inverted Multiphoton Microscope (A1MP + Eclipse Ti-2E, Nikon instrument Inc., Japan) with a 40 x NA = 1.15 water-immersion objective. A laser with wavelength-tunable (700 – 1300 nm) near-infrared femtosecond laser (Insight X3, Spectra-Physics) served as the light source for two-photon fluorescence imaging. The time-correlated single-photon counting system (SPC-160, Becker& Hickl) was used to measure and calculate lifetime. The luminescence signals were two-photon excited at 800 nm and collected in the range of 550 – 650 nm. Photoluminescence lifetime images with 512 x 512 pixels were acquired with scan speed of 30 Hz. The images were recorded after an excitation pulse without any time delay. Finally, the PLIM data were analyzed using a pixel-based fitting software (SPCImage, Becker & Hickl). An incomplete decay model in SPCImage software was employed for the calculation of lifetime for **K293** and nitroxoline.

2.4. BRD4 knockdown assay

A375 cells were seeded in 6-well plates at 75% confluence in culture medium for 24 h. Lipo3000 reagent and BRD4 siRNA (GUGCUGAUGUCCGAUUGAU) was gently mixed and incubated together for 15 min at room temperature. The medium of the cells was replaced with fresh medium, and 500 μL of the Lipo3000 / siRNA mixture were added to each well. Cells were incubated at 37 °C in a CO_2 incubator for 48 h post-transfection before use.

2.5. Immunofluorescence

A375 cells were initially washed three times using PBS buffer.

Afterwards, 4% paraformaldehyde (PFA) was added and the cells were incubated for 30 min, followed by triplicate washing with PBS. Next, 0.5% Triton X-100 was added and the cells were incubated at room temperature for 30 min, followed by washing with PBS buffer three times. After blocking with 5% BSA for 30 min, the cells were incubated with the primary BRD4 antibody overnight incubation at 4 °C and then subsequently with secondary antibody for 2 h at ambient temperature. The images were captured using Leica TCS SP8 confocal laser scanning microscope.

3. Results and discussion

3.1. Synthesis of K293 probe

K197 is an effective natural product-like BRD4 inhibitor developed previously by our group [13]. To design the luminescent **K293** probe, the inhibitor **K197** was connected to an iridium scaffold through an alkyl chain, which eliminating the potential disturbance of the iridium complex to the binding affinity of **K197**. **K293** probe was prepared in four steps (Fig. 1). Ligand 1 was reacted with (*tert*-butoxycarbonyl) glycine in the presence of dicyclohexylcarbodiimide (DCC) to generate a Boc-protected intermediate, which was directly deprotected with trifluoroacetic acid (TFA) treatment to give compound 2. Compound 2 was then coupled with reagent 3 using 1-ethyl-3-(3-dimethylaminopropyl) carbod-iimide hydrochloride (EDCI), 1-hydroxybenzotriazole (HOBt) and triethylamine (Et_3N) to produce ligand 4, which was subsequently reacted with the dimer $Ir_2(ppy)_4Cl_2$ (where ppy = 2-phenylpyridine) to obtain iridium(III) complex 5. Complex 5 was then treated by TFA, followed by the reaction with **K197** in the presence of EDCI, HOBt and Et_3N, which was then followed by another round of deprotection with TFA to yield **K293**. All intermediates and **K293** were fully characterized by ^1H NMR and ^{13}C NMR and high-resolution mass spectrometry (HRMS) (Figs. S1-S14).

3.2. Photophysical properties of K293 probe

The photophysical properties of **K293** *in vitro* were further explored. **K293** showed a higher quantum yield (*ca.* 0.193) using $Ru(bpy)_3$ (bpy = 2,2′-bipyridine) (*ca.* 0.062) as a standard (Fig. S15). **K293** showed a maximum excitation wavelength at 420 nm and a maximum emission wavelength at 590 nm (Fig. S16A). Importantly, **K293** probe displayed a wide Stokes shift of 270 nm, which helps to reduce self-quenching. Moreover, **K293** probe exhibited a long-lived phosphorescence lifetime of 862 ns (Fig. S16B). This indicates that **K293** shows high photostability in living cells.

Iridium complexes exhibit a long-lived phosphorescence lifetime, allowing their emission to be discriminated from a fluorescent background by the use of time-resolved emission spectroscopy (TRES). As a proof-of-concept experiment, coumarin 460 (Cm460), an organic dye, was chosen to mimic the autofluorescence of biological samples. Under steady state conditions (decay 0 ns), Cm460 produces a strong emission peak at 460 nm with a tail extending to 700 nm, which interferes with the luminescence emission of **K293** (Fig.S16C). However, in TRES mode (decay 333 ns), the luminescence emission of Cm460 is completely eliminated allowing the signal from **K293** to be clearly detected at 590 nm (Fig.S16D). Finally, the luminescence intensity of **K293** in A375 cells decreased only gradually under continuous excitation at 405 nm over 1000 s, whereas the well-known organic dye DAPI suffered a large decrease in luminescence intensity under the same conditions (Figs. S17A and S17B). Hence, the use of TRES can improve the sensitivity of a screening platform as well as help to prevent false positive or negative screening results.

3.3. The binding ability of K293 probe in vitro

The cellular thermal shift assay (CETSA) was performed to determine the ability of **K293** probe to engage BRD4 in cell lysates. A375 cell lysates were treated with the different concentrations (0, 2, 5, 10, 20, 50, 100 μM) of **K293** probe or the well-known BRD4 inhibitor JQ1 for 30 min at room temperature. The results showed that both JQ1 and **K293** can stabilize BRD4 in A375 cell lysates in a dose-dependent manner (Fig. 2A and 2B). The CETSA data revealed K_d values of 44.2 μM and 1.39 μM for the binding of **K293** and JQ1 to BRD respectively, indicating that both **K293** and JQ1 could stabilize the BRD4 protein. Moreover, molecular modeling was also performed to elucidate the binding mode of **K293** binding unit, **K197**, and Azelastine with BRD4, which based on

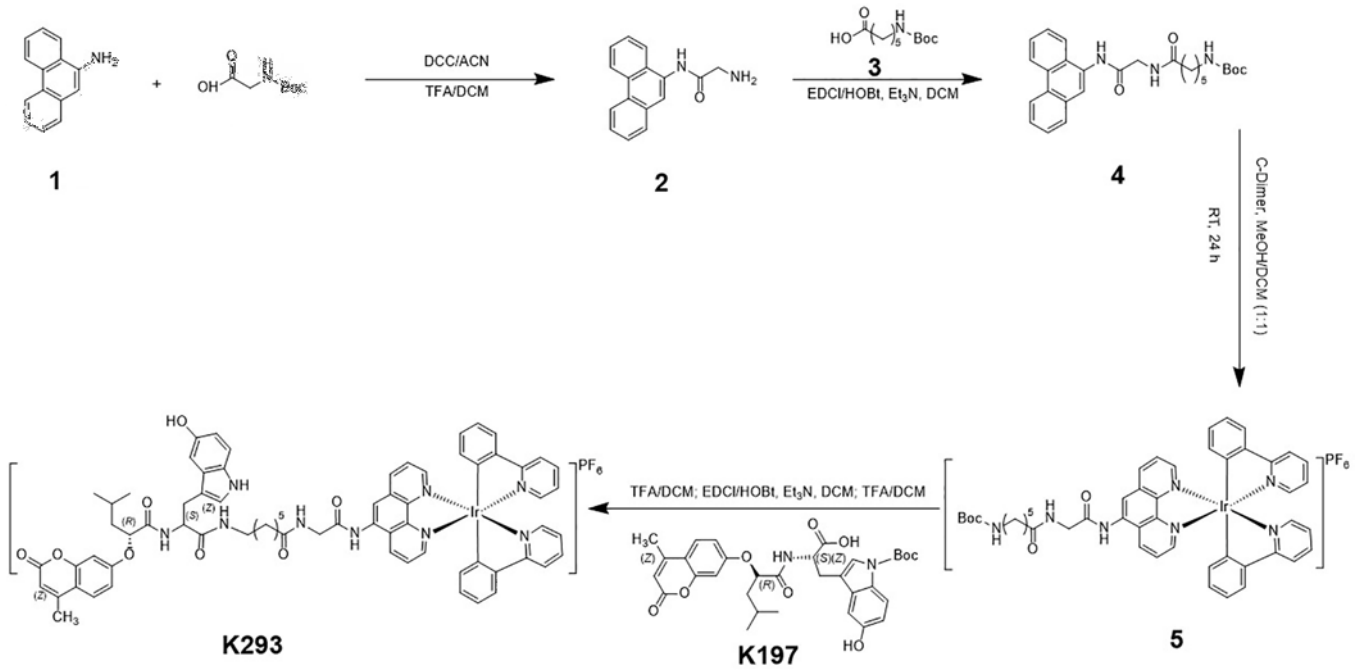

Fig. 1. Synthesis route of probe **K293**. Reagents and conditions: a) DCC, ACN, then TFA, DCM; b) EDCI, HOBt, Et_3N, DCM; c) $Ir_2(ppy)_4Cl_2$ dimer, MeOH/DCM (1/1); d) TFA, DCM, then EDCI, HOBt, Et_3N, followed by TFA, DCM.

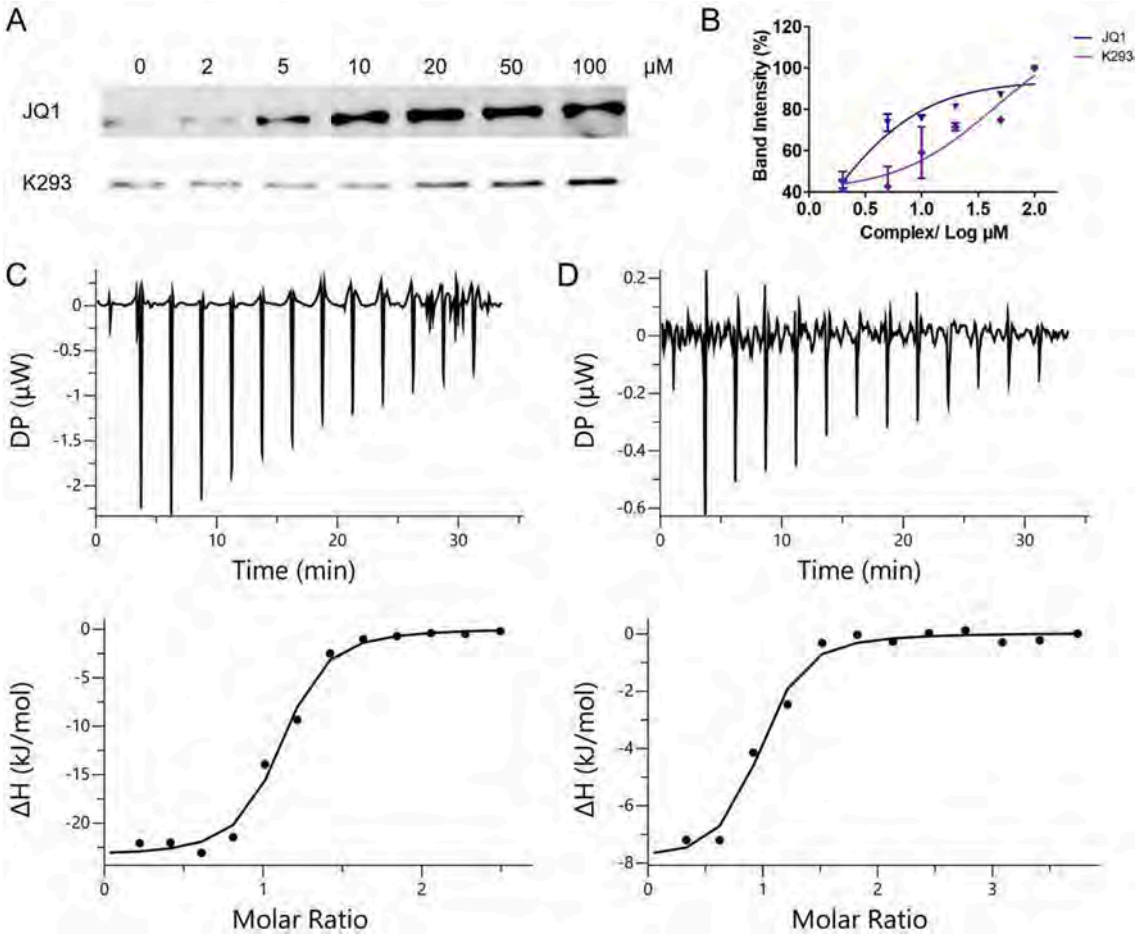

Fig. 2. **K293** could bind with BRD4 protein. (A) CETSA for the binding of **K293** probe and JQ1 (0 – 100 μM) to BRD4 in cell lysate. (B) Densitometry analysis of CETSA for the level of remaining soluble protein of BRD4 at different incubation concentrations for **K293** or JQ1-treated control samples. (C) ITC titration of **K293** (200 μM) into recombinant BRD4 BD1 protein (20 μM) and (D) BRD4 BD2 protein (20 μM). ITC experiments were carried out in a MicroCal PEAQ-ITC isothermal titration calorimeter (Malvern Panalytical).

X-ray crystal structure of BRD4 with a well-known BRD4 inhibitor, A-1457066. Similarly, **K197** and Azelastine occupied the main pocket of A-1457066 located. But the minor difference is that linear **K197** extends into another cavity with two H-bond interaction with backbone and sidechain of Lys378 (Fig.S18).

Isothermal titration calorimetric (ITC) analysis was then conducted to investigate the thermodynamics of the interaction between **K293** and the BD1 and BD2 domains of BRD4 (Fig. 2C and 2D). The stoichiometry of the interaction was determined to be $N = 1.03 \pm 0.027$ for BD1 and $N = 0.864 \pm 0.042$ for BD2, while the binding affinities were determined to be $K_d = 0.270 \pm 0.011$ μM and $K_d = 0.381 \pm 0.019$ μM for BD1 and BD2 respectively. The thermodynamic parameters of binding also indicated that the binding between **K293** and BRD4 is both enthalpically and entropically-driven (BD1: $\Delta H = -23.6 \pm 1.17$ kcal/mol, $\Delta G = -37.5$ kcal/mol, $-T\Delta S = -14.0$ kcal/mol; BD2: $\Delta H = -8.04 \pm 0.641$ kcal/mol, $\Delta G = -36.7$ kcal/mol, $-T\Delta S = -28.6$ kcal/mol).

3.4. Biocompatibility and imaging ability of K293 probe in cellulo

An ideal cellular imaging probe should possess no or very little toxicity in cells. To study the toxicity of **K293**, a 3-(4,5-dimethylthiazol-2-yl)-2,5-diphenyltetrazolium bromide (MTT) assay was performed in the melanoma cell line A375 and the normal liver cell line LO2. Encouragingly, **K293** probe showed minimal cytotoxicity against both A375 and LO2 cell lines (Fig. S19). This indicates the luminescence changes observed in the cell imaging experiments are not affected by changes of cell proliferation.

We first optimized the imaging ability of **K293** in A375 cells. A375 was used as the model cell line as it is known to overexpress BRD4 protein [25]. Before imaging, cells were washed three times with PBS to remove non-specific binding. The results showed emission signal of **K293** in A375 cells increased in a dose-dependent (Fig. S20) and time-dependent manner (Fig. S21), with 5 μM of **K293** and 2 h incubation time giving the best imaging performance in the cytoplasm.

To investigate the imaging performance of the probe, A375 cells were incubated with either DMSO or **K293** under the optimized conditions. The cells treated with DMSO were non-luminescent (Fig. S22a). Encouragingly, cells treated with **K293** showed distinct emission (Fig. S22b). Then, to further investigate the potential of **K293** for screening BRD4 inhibitors, A375 cells were co-treated with BRD4 inhibitors **N13** or JQ1 (5 μM) and **K293** (5 μM) for 2 h (Figs. S22c and S22d). Cells were washed three times with PBS to remove non-specific binding before imaging. The results revealed that as the concentration of BRD4 inhibitors JQ1 and **N13** increases, the luminescence of **K293** in the cells diminishes. In order to assess whether the **K293** probe can be used to study the potency of compounds, we performed a dose-dependent assay with Azelastine (Fig. S23). The result indicated that as the concentration of Azelastine increases, the luminescence of the system gradually decreases. We expect that the competitive binding of the inhibitors to BRD4 decreases the binding of **K293** to the protein. Subsequently, the unbound probe is removed in the buffer wash, thereby resulting in a decrease in luminescence.

To further confirm that **K293** is a specific BRD4 probe, knockdown experiments were performed. We first verified that BRD4 protein levels in A375 cells were significantly decreased by BRD4 siRNA through Western blotting (Fig. S24). In the imaging experiments, the luminescence of **K293** was significantly decreased in BRD4 knockdown A375 cells compared to control cells without BRD4 knockdown treated with siControl (Fig. 3A), suggesting that the binding to BRD4 is required for the generation of the emission signal in the cytoplasm. To further confirm that the retention of probe **K293** in A375 cells is due to binding to BRD4, ICP-MS experiments were performed. The results showed that BRD4 knockdown cells treated with **K293** retained lower levels of iridium after washing compared to control cells, consistent with the reduced binding of **K293** probe in the absence of BRD4 (Fig. S25). Taken together, experiments demonstrate that BRD4 is the target of **K293** *incellulo*.

We also investigated the imaging performance of **Ir_C13**, which possesses the same emissive metal scaffold as **K293** but lacks the binding moiety of **K293** (Fig. 3B). A375 cells treated with siBRD4 or siControl were then incubated with **Ir_C13** for 2 h. As shown in Fig. 3A, there are no significant luminescence changes of **Ir_C13** in siBRD4 or siControl cells. This is because **Ir_C13** lacks BRD4 targeting ability, and hence shows the same luminescence in cells regardless of whether or not BRD4 is present. This result further supports the hypothesis that the binding of **K293** to BRD4 *in cellulo* is required for the enhanced luminescence of the probe in A375 cells.

Given the ability of **K293** probe to target BRD4, we further explored whether **K293** could affect the translocation of BRD4 from the cytoplasm to the nucleus *in cellulo*. A375 cells were treated with either DMSO, JQ1 (5 μM) or **K293** probe (5 μM) for 2 h. After washing three times with PBS to remove non-specific binding, the distribution of BRD4 protein was visualized by immunofluorescence with anti-BRD4 antibodies (Fig. 3C). In control group, BRD4 was mainly concentrated in the nucleus of the cell. Interestingly, both **K293** and JQ1 could decrease the translocation of BRD4 into the nucleus, as indicated by the presence of stronger luminescence in the cytoplasm compared to the control group.

In order to study the selectivity of the **K293** probe, we detected the relationship between the **K293** probe and the other BET family members BRD2 and BRD3. The CETSA assay was performed and found that the **K293** probe could only significantly stabilized BRD4 in A375 cell lysates instead of the BRD2, BRD3 or β-actin (Fig. S26A), suggesting that the **K293** probe could engage BRD4 within cells. Moreover, to further confirmed the selective ability, the BRD2, BRD3 and BRD4 were knockdown using the related siRNA and then western blot and confocal imaging assay were performed. As shown in Fig. S26B and S26C, the luminescence was clearly decreased only when BRD4 was knocked down. In contrast, the luminescence of other BET family proteins did not change significantly after they were knocked down. Therefore, the above results demonstrated that the **K293** is a BRD4-selective probe.

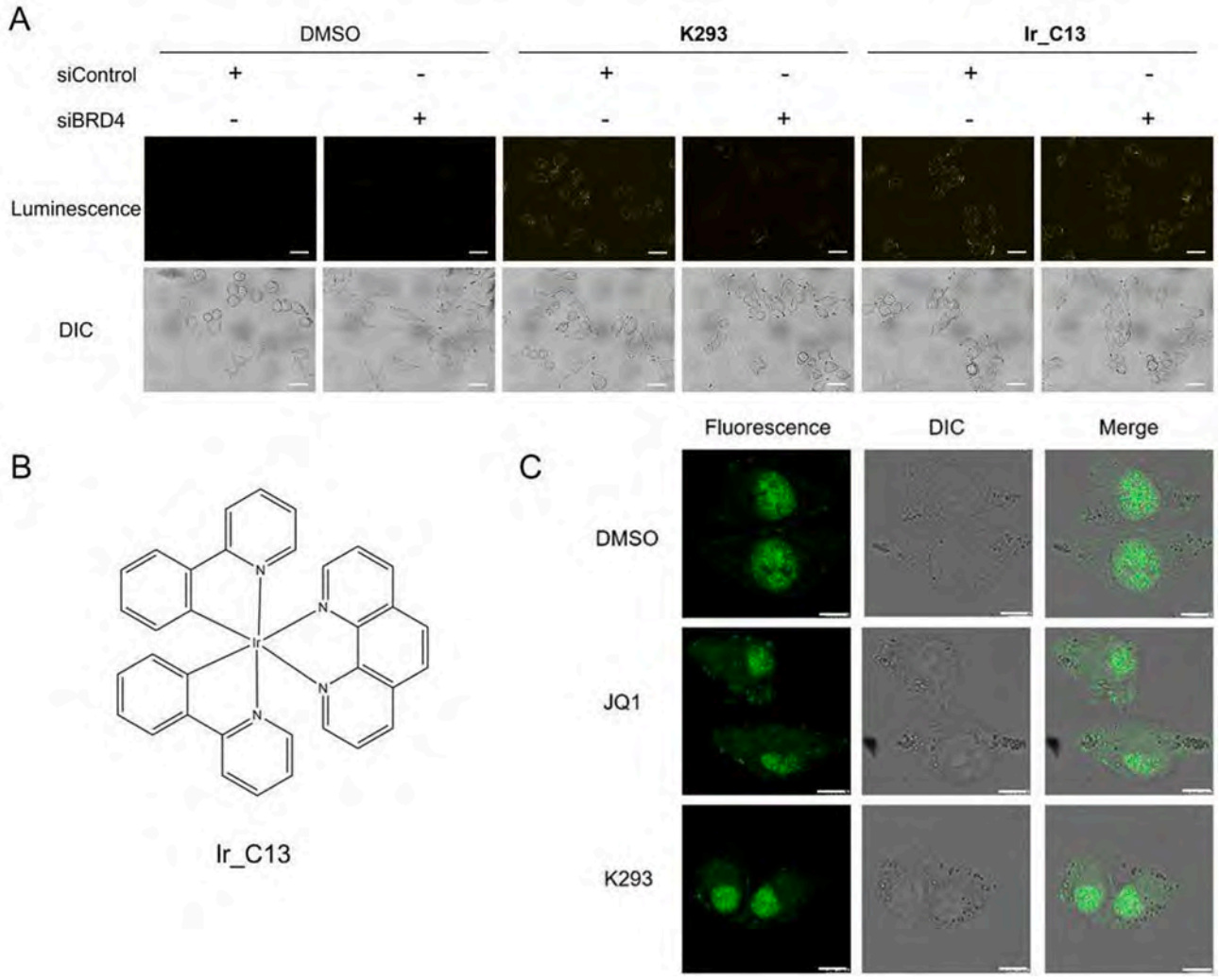

Fig. 3. Luminescence images in A375 cells. (A) A375 cells were incubated with siControl or siBRD4 for 48 h and then treated with 5 μM **K293** or Ir_C13 for 2 h. Cell images were detected at λexc/λemi = 405/500 – 700 nm. Scale bar: 100 μm. (B) The chemical structure of Ir_C13. (C) Immunofluorescence studies of JQ1 or **K293** probe with BRD4 antibody in A375 cells. The luminescence was detected at λexc/λemi = 488/500 – 700 nm. Scale bar = 25 μm.

To demonstrate the advantage of the long luminescence lifetime of transition metal complexes, **K293**-stained A375 cells were visualized using phosphorescence lifetime imaging microscopy (PLIM). Most of the background fluorescence has a luminescence lifetime of less than 3 ns, which is much shorter than the phosphorescence lifetime of iridium(III) complexes, including **K293** (862 ns). This large difference allows the temporal discrimination of the probe signal from the strong background fluorescence of cells. As shown in Fig. S27, the long lifetime of complex **K293** in the cell boundaries and the cytoplasm (green color) of A375 cells could be detected using PLIM. In contrast, Nitroxoline, an FDA-approved antibiotic [26,27] that has previously been reported as a BRD4 inhibitor [28,29], displayed a much shorter lifetime than the temporal resolution of PLIM in the cell (orange color). The PLIM results confirm that **K293** displays a much longer apparent lifetime within cells than fluorescent compounds, indicating that **K293** could be suitable for long-lived luminescence imaging even in the presence of an endogenous fluorescence background signal.

3.5. K293 probe-based BRD4 inhibitor screening platform

To perform the BRD4 inhibitor screening assay, A375 cells were incubated with both **K293** probe (5 μM) and candidate compounds (5 μM) for 2 h. After washing with PBS buffer three times to remove non-specific binding, cell images were recorded. As a proof-of concept, 500 FDA-approved drugs were screened using the platform (Fig. 4A). From the screening results, Azelastine emerged as a potential BRD4 inhibitor. The cell images clearly showed a decrease in the luminescence of **K293** in the presence of Azelastine, indicating that Azelastine may be a potential inhibitor of BRD4 (Fig. 4B). We confirmed the BRD4 inhibitory activity of Azelastine using a commercially available BRD4 TR-FRET assay kit, where it showed slightly lower potency than JQ1 (Fig. S28). Moreover, Azelastine significantly stabilized BRD4 in A375 cell lysates compared to the DMSO control in a CETSA experiment (Fig. 4C and 4D), suggesting that Azelastine could engage BRD4 within cells. These results demonstrate that our screening platform can be used to successfully identify potential BRD4 inhibitors.

3.6. Azelastine blocks the translocation of BRD4 into the nucleus and inhibits the viability, migration and cell cycle of melanoma cells

We next investigated the biological activities of Azelastine using a range of cellular assays. After treatment of A375 cells with Azelastine or JQ1, the distribution of BRD4 in the cytoplasm was significantly increased, while the distribution of BRD4 in the nucleus was reduced as shown by Western blotting (Fig. 5A). These results suggest that Azelastine can inhibit the translocation of BRD4 from the cytoplasm into the nucleus. The toxicity of Azelastine in A375 and LO2 cells was also tested by the MTT assay. Azelastine inhibited the viability of A375 melanoma cells with an IC_{50} value of 16.0 μM, suggesting that it displays moderate anticancer activity (Fig. 5B). To determine the impact of Azelastine on A375 cell migration, the wound healing assay was performed. A dose of 5 μM Azelastine or JQ1 treatment effectively inhibited the migration of

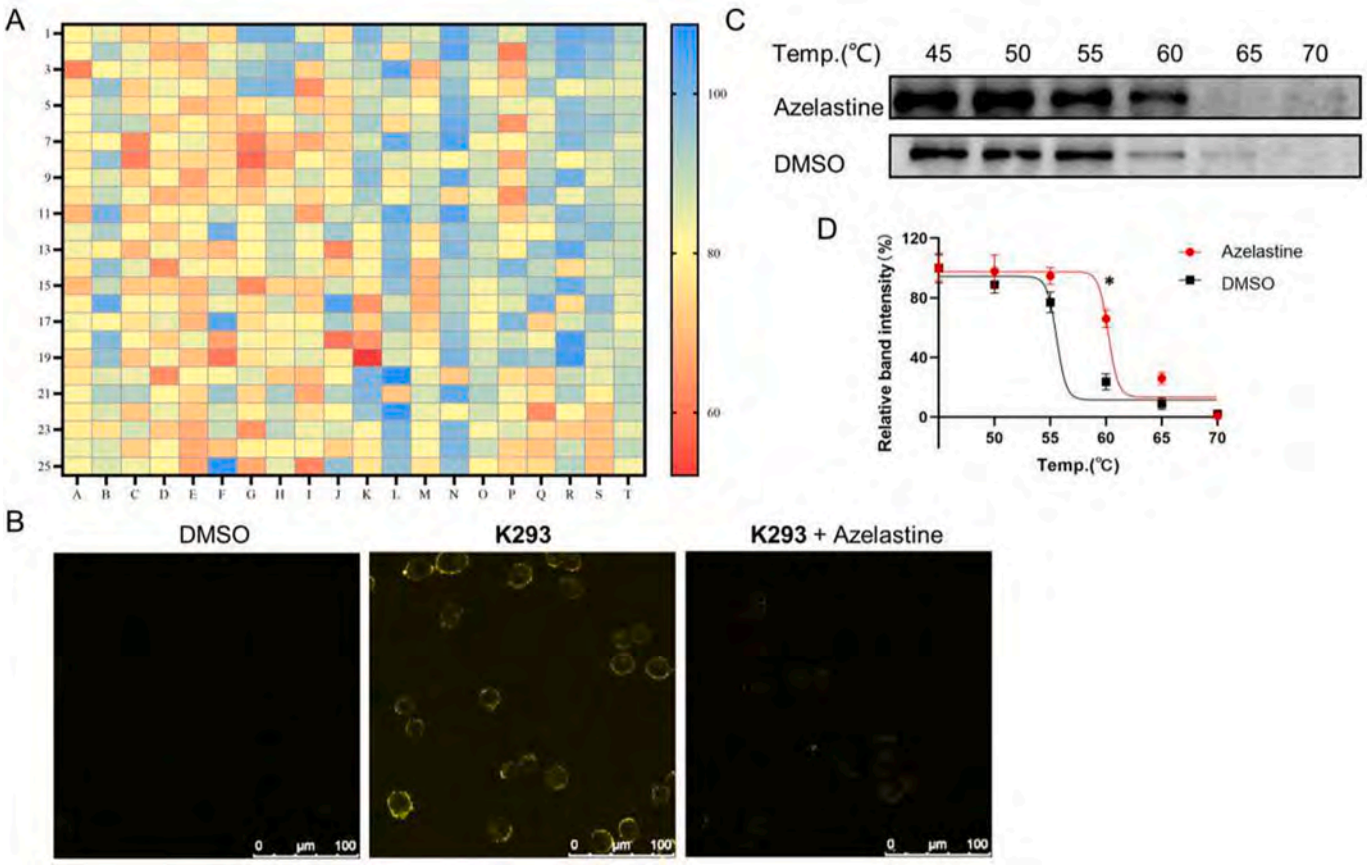

Fig. 4. Azelastine is a potential BRD4 inhibitor. (A) Confocal drug screening assay based on the **K293** probe. A375 cells were incubated with FDA-approved drugs (5 μM) and **K293** probe (5 μM) for 2 h. The luminescence signal in cells was detected using confocal microscope. The luminescence signals of the FDA-approved drugs in treatment groups were compared with the **K293** probe positive group. (B) Luminescence imaging of A375 cells treated with 5 μM Azelastine and incubated with **K293** probe, images were taken under a confocal microscope. The luminescence was detected at λexc/λemi = 405/500 –700 nm. Scale bar = 100 μm. (C) Stabilization of BRD4 by Azelastine *in cellulo*. A375 cell lysates were treated with 10 μM of Azelastine or DMSO at room temperature for 30 min and then heated at different temperatures ranging from 45 to 70 °C for 8 min. The supernatants of protein samples were collected and detected by Western blotting using BRD4 antibody. (D) Densitometry analysis of BRD4 content in the soluble fraction. *p less than 0.05 compared to DMSO group by the t-test.

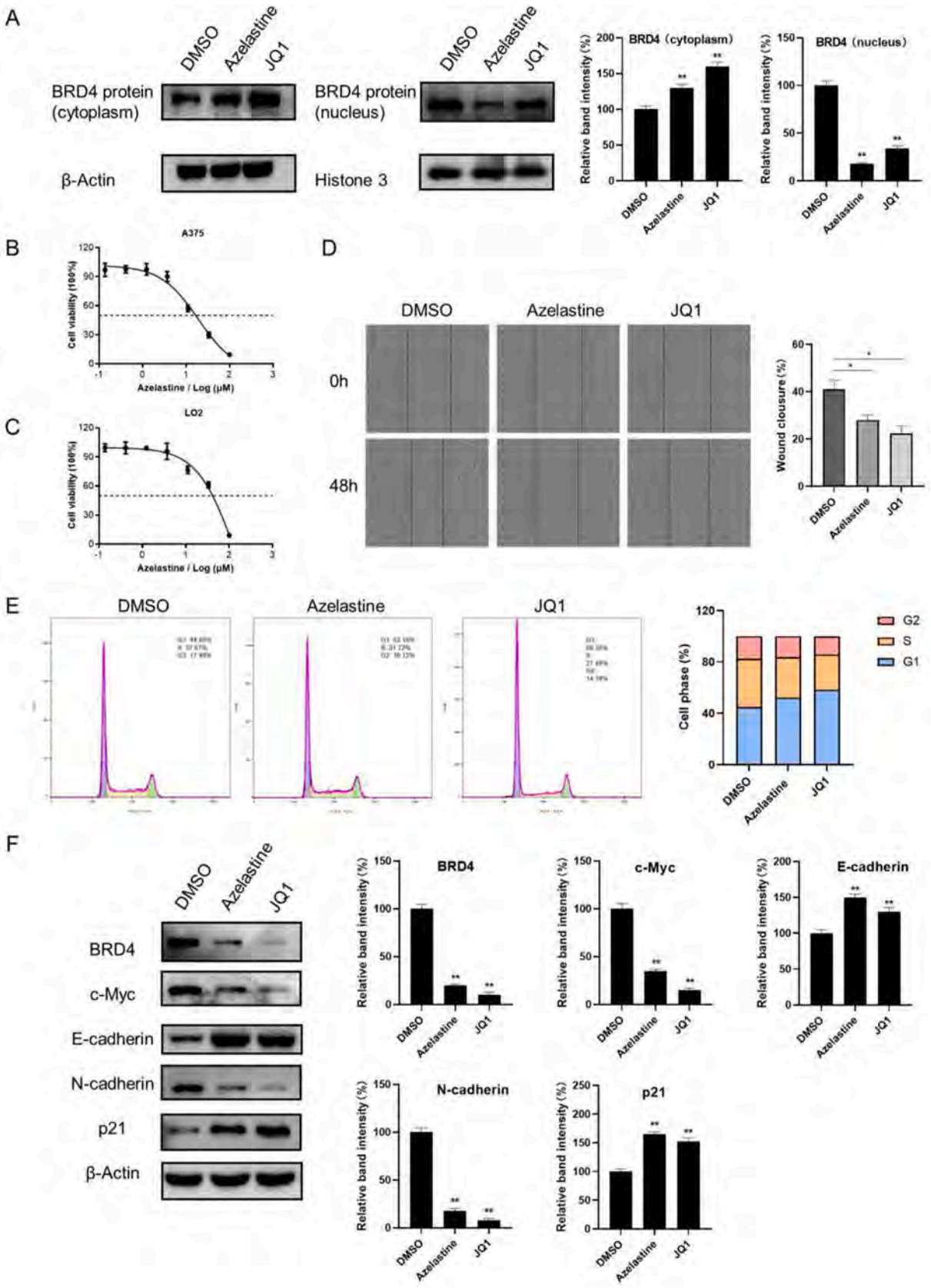

Fig. 5. Azelastine inhibits the cell viability, migration and cell cycle of A375 melanoma cells. (A) Azelastine can inhibit the translocation of BRD4 protein into the nucleus. (B-C) Azelastine could inhibit the viability of A375 melanoma and LO2 cells. (D) Azelastine could inhibit the migration of A375 melanoma cells. (E) A375 cells were incubated with 5 μM Azelastine or JQ1 for 12 h, collected and subjected to cell cycle analysis. The bar graph represents the mean percentage of cells at each of the cell cycle phases. (F) Protein levels of BRD4, c-Myc, E-cadherin, N-cadherin, p21 and β-Actin in A375 cells treated with Azelastine or JQ1 were measured by Western blot.

A375 cells compared with the control group (Fig. 5C). In the cell cycle arrest assay, Azelastine-treated A375 cells showed an increase in the population of G_0/G_1 phase cells and a decrease in the population of S phase cells (Fig. 5D). This result indicates that Azelastine induces G_0/G_1 cell-cycle arrest in A375 cells. In addition, A375 cells treated with Azelastine or JQ1 showed reduced BRD4, c-Myc and N-cadherin expression and increased E-cadherin and p21 expression (Fig. 5E). This result indicates that Azelastine inhibits the EMT process in A375 cells. We anticipate that the inhibition of A375 cell proliferation, migration and EMT is due, at least in part, to the ability of Azelastine to engage BRD4 and inhibit its activity in cells.

4. Conclusions

In summary, the iridium-based **K293** was developed as a selective and non-toxic probe for the imaging of BRD4 in living cells to screen potential BRD4 inhibitors which are undetectable by traditional methods. Because of its promising biocompatibility, long lifetime, and BRD4 response with excellent selectivity, **K293** can be used as a BRD4 probe to evaluate BRD4 activity upon treatment with anti-cancer drugs. Using **K293**, a luminescence screening platform was developed for screening BRD4 inhibitors for cancer treatment. As a proof-of-concept, 500 FDA-approved compounds were screened using this platform which led to the identification of Azelastine as a BRD4 inhibitor in cancer cells. We anticipate that this study could facilitate the development of more luminescence-based screening platforms identify new pharmacological agents for treating different kinds of cancer, as well as further highlight the benefit of repurposing existing drugs against cancer.

Declaration of Competing Interest

The authors declare that they have no known competing financial interests or personal relationships that could have appeared to influence the work reported in this paper.

Data availability

Data will be made available on request.

Acknowledgments

This work is supported by the Science and Technology Development Fund (Macau SAR, China) (0007/2020/A1, 0020/2022/A1, SKL-QRCM (UM)-2023-2025), the University of Macau (China) (MYRG2020-00017-ICMS, MYRG2022-00137-ICMS), 2022 Internal Research Grant of SKL-QRCM (University of Macau) (QRCM-IRG2022-011), the National Natural Science Foundation of China (22101230, 22077109, 21775131), the Natural Science Basic Research Program of Shaanxi (2021JQ-089), the Natural Science Foundation of Chongqing, China (cstc2021jcyj-msxmX0659), the HKBU SKLEBA Research Grant (SKLP_2223_P03).

Appendix A. Supplementary data

Supplementary data to this article can be found online at https://doi.org/10.1016/j.cej.2023.142356.

References

[1] P. Filippakopoulos, J. Qi, S. Picaud, Y. Shen, W.B. Smith, O. Fedorov, E.M. Morse, T. Keates, T.T. Hickman, I. Felletar, M. Philpott, S. Munro, M.R. McKeown, Y. Wang, A.L. Christie, N. West, M.J. Cameron, B. Schwartz, T.D. Heightman, N. La Thangue, C.A. French, O. Wiest, A.L. Kung, S. Knapp, J.E. Bradner, Selective inhibition of BET bromodomains, Nature 468 (7327) (2010) 1067–1073, https://doi.org/10.1038/nature09504.

[2] M.K. Jang, K. Mochizuki, M. Zhou, H.S. Jeong, J.N. Brady, K. Ozato, The bromodomain protein Brd4 is a positive regulatory component of P-TEFb and stimulates RNA polymerase II-dependent transcription, Mol. Cell 19 (4) (2005) 523–534, https://doi.org/10.1016/j.molcel.2005.06.027.

[3] I.A. Asangani, V.L. Dommeti, X. Wang, R. Malik, M. Cieslik, R. Yang, J. Escara-Wilke, K. Wilder-Romans, S. Dhanireddy, C. Engelke, M.K. Iyer, X. Jing, Y.M. Wu, X. Cao, Z.S. Qin, S. Wang, F.Y. Feng, A.M. Chinnaiyan, Therapeutic targeting of BET bromodomain proteins in castration-resistant prostate cancer, Nature 510 (7504) (2014) 278–282, https://doi.org/10.1038/nature13229.

[4] Z. Zou, B. Huang, X. Wu, H. Zhang, J. Qi, J. Bradner, S. Nair, L.F. Chen, Brd4 maintains constitutively active NF-κB in cancer cells by binding to acetylated RelA, Oncogene 33 (18) (2014) 2395–2404, https://doi.org/10.1038/onc.2013.179.

[5] G.J. Yang, W. Wang, P.M. Lei, C.H. Leung, D.L. Ma, A 7-methoxybicoumarin derivative selectively inhibits BRD4 BD2 for anti-melanoma therapy, Int. J. Biol. Macromol. 164 (2020) 3204–3220, https://doi.org/10.1016/j.ijbiomac.2020.08.194.

[6] C. Luo, J.H. Lim, Y. Lee, S.R. Granter, A. Thomas, F. Vazquez, H.R. Widlund, P. Puigserver, A PGC1alpha-mediated transcriptional axis suppresses melanoma metastasis, Nature 537 (7620) (2016) 422–426, https://doi.org/10.1038/nature19347.

[7] Y.F. Zheng, Y.Q. Wu, B.Y. Hu, L.C. Tao, C. Xi, H. Dixon, F.L. Hu, Chrysin inhibits melanoma tumor metastasis via interfering with the FOXM1/beta-catenin signaling, J. Agric. Food Chem. 68 (35) (2020) 9358–9367, https://doi.org/10.1021/acs.jafc.0c03123.

[8] N. Pencheva, H. Tran, C. Buss, D. Huh, M. Drobnjak, K. Busam, S.F. Tavazoie, Convergent multi-miRNA targeting of ApoE drives LRP1/LRP8-dependent melanoma metastasis and angiogenesis, Cell 151 (5) (2012) 1068–1082, https://doi.org/10.1016/j.cell.2012.10.028.

[9] A. Sadok, A. McCarthy, J. Caldwell, I. Collins, M.D. Garrett, M. Yeo, S. Hooper, E. Sahai, S. Kuemper, F.K. Mardakheh, C.J. Marshall, Rho kinase inhibitors block melanoma cell migration and inhibit metastasis, Cancer Res. 75 (11) (2015) 2272–2284, https://doi.org/10.1158/0008-5472.CAN-14-2156.

[10] P. Zhang, R. Li, H. Xiao, W. Liu, X. Zeng, G. Xie, W. Yang, L. Shi, Y. Yin, K. Tao, BRD4 inhibitor AZD5153 suppresses the proliferation of colorectal cancer cells and sensitizes the anticancer effect of PARP inhibitor, Int. J. Biol. Sci. 15 (9) (2019) 1942–1954, https://doi.org/10.7150/ijbs.34162.

[11] S. Shu, H.-J. Wu, J.Y. Ge, R. Zeid, I.S. Harris, B. Jovanović, K. Murphy, B. Wang, X. Qiu, J.E. Endress, J. Reyes, K. Lim, A. Font-Tello, S. Syamala, T. Xiao, C.S. Reddy Chilamakuri, E.K. Papachristou, C. D'Santos, J. Anand, K. Hinohara, W. Li, T. O. McDonald, A. Luoma, R.J. Modiste, Q.-D. Nguyen, B. Michel, P. Cejas, C. Kadoch, J.D. Jaffe, K.W. Wucherpfennig, J. Qi, X.S. Liu, H. Long, M. Brown, J. S. Carroll, J.S. Brugge, J. Bradner, F. Michor, K. Polyak, Synthetic lethal and resistance interactions with BET bromodomain inhibitors in triple-negative breast cancer, Molecular Cell 78 (6) (2020) 1096–1113.e8.

[12] P. Zhang, D. Wang, Y. Zhao, S. Ren, K. Gao, Z. Ye, S. Wang, C.W. Pan, Y. Zhu, Y. Yan, Y. Yang, D. Wu, Y. He, J. Zhang, D. Lu, X. Liu, L. Yu, S. Zhao, Y. Li, D. Lin, Y. Wang, L. Wang, Y. Chen, Y. Sun, C. Wang, H. Huang, Intrinsic BET inhibitor resistance in SPOP-mutated prostate cancer is mediated by BET protein stabilization and AKT-mTORC1 activation, Nat. Med. 23 (9) (2017) 1055–1062, https://doi.org/10.1038/nm.4379.

[13] G.J. Yang, Y.Q. Song, W. Wang, Q.B. Han, D.L. Ma, C.H. Leung, An optimized BRD4 inhibitor effectively eliminates NF-κB-driven triple-negative breast cancer cells, Bioorg. Chem. 114 (2021), 105158, https://doi.org/10.1016/j.bioorg.2021.105158.

[14] F.N. Guo, Y.T. Wang, N. Wu, L.X. Feng, H.C. Zhang, T. Yang, J.H. Wang, Carbon nitride nanoparticles as ultrasensitive fluorescent probes for the detection of alpha-glucosidase activity and inhibitor screening, Analyst 146 (3) (2021) 1016–1022, https://doi.org/10.1039/d0an02079f.

[15] M. Shi, Y. Cen, G. Xu, F. Wei, X. Xu, X. Cheng, Y. Chai, M. Sohail, Q. Hu, Ratiometric fluorescence monitoring of alpha-glucosidase activity based on oxidase-like property of MnO2 nanosheet and its application for inhibitor screening, Anal. Chim. Acta 1077 (2019) 225–231, https://doi.org/10.1016/j.aca.2019.05.037.

[16] D.L. Ma, C. Wu, H. Liu, K.J. Wu, C.H. Leung, Luminescence approaches for the rapid detection of disease-related receptor proteins using transition metal-based probes, J. Mater. Chem. B 8 (16) (2020) 3249–3260, https://doi.org/10.1039/c9tb01889a.

[17] M.D. Hall, A. Yasgar, T. Peryea, J.C. Braisted, A. Jadhav, A. Simeonov, N. P. Coussens, Fluorescence polarization assays in high-throughput screening and drug discovery: a review, Methods Appl. Fluoresc. 4 (2) (2016), 022001, https://doi.org/10.1088/2050-6120/4/2/022001.

[18] A. Jiang, Y. Liu, G. Chen, Y. Li, B. Tang, The cross-talk modulation of excited state electron transfer to reduce the false negative background for high fidelity imaging in vivo, Chem. Sci. 11 (7) (2020) 1964–1974, https://doi.org/10.1039/c9sc05765j.

[19] K.L. Vedvik, H.C. Eliason, R.L. Hoffman, J.R. Gibson, K.R. Kupcho, R.L. Somberg, K.W. Vogel, Overcoming compound interference in fluorescence polarization-based kinase assays using far-red tracers, Assay Drug Dev. Technol. 2 (2) (2004) 193–203, https://doi.org/10.1089/154065804323056530.

[20] S. Tobita, T. Yoshihara, Intracellular and in vivo oxygen sensing using phosphorescent iridium(III) complexes, Curr. Opin. Chem. Biol. 33 (2016) 39–45, https://doi.org/10.1016/j.cbpa.2016.05.017.

[21] K.Y. Zhang, T. Zhang, H. Wei, Q. Wu, S. Liu, Q. Zhao, W. Huang, Phosphorescent iridium(iii) complexes capable of imaging and distinguishing between exogenous and endogenous analytes in living cells, Chem. Sci. 9 (36) (2018) 7236–7240, https://doi.org/10.1039/c8sc02984a.

[22] K.J. Wu, S.H. Ho, J.Y. Dong, L. Fu, S.P. Wang, H. Liu, C. Wu, C.H. Leung, H. D. Wang, D.L. Ma, Aliphatic group-tethered iridium complex as a theranostic agent

against malignant melanoma metastasis, ACS Appl. Bio Mater. 3 (4) (2020) 2017–2027, https://doi.org/10.1021/acsabm.9b01156.
[23] W. Wang, K.J. Wu, K. Vellaisamy, C.H. Leung, D.L. Ma, Peptide-conjugated long-lived theranostic imaging for targeting GRPr in cancer and immune cells, Angew Chem Int Ed Engl 59 (41) (2020) 17897–17902, https://doi.org/10.1002/anie.202007920.
[24] R.A. Blake, Cellular screening assays using fluorescence microscopy, Curr Opin Pharmacol 1 (5) (2001) 533–539, https://doi.org/10.1016/s1471-4892(01)00092-3.
[25] M. Yin, Y. Guo, R. Hu, W.L. Cai, Y. Li, S. Pei, H. Sun, C. Peng, J. Li, R. Ye, Q. Yang, N. Wang, Y. Tao, X. Chen, Q. Yan, Potent BRD4 inhibitor suppresses cancer cell-macrophage interaction, Nat. Commun. 11 (1) (2020) 1183, https://doi.org/10.1038/s41467-020-15290-0.
[26] J. Lazovic, L. Guo, J. Nakashima, L. Mirsadraei, W. Yong, H.J. Kim, B. Ellingson, H. Wu, W.B. Pope, Nitroxoline induces apoptosis and slows glioma growth in vivo, Neuro-oncology 17 (1) (2015) 53–62, https://doi.org/10.1093/neuonc/nou139.
[27] J. Xing, R. Zhang, X. Jiang, T. Hu, X. Wang, G. Qiao, J. Wang, F. Yang, X. Luo, K. Chen, J. Shen, C. Luo, H. Jiang, M. Zheng, Rational design of 5-((1H-imidazol-1-yl)methyl)quinolin-8-ol derivatives as novel bromodomain-containing protein 4 inhibitors, Eur. J. Med. Chem. 163 (2019) 281–294, https://doi.org/10.1016/j.ejmech.2018.11.018.
[28] G. Li, Y.H. Zheng, L. Xu, J. Feng, H.L. Tang, C. Luo, Y.P. Song, X.Q. Chen, BRD4 inhibitor nitroxoline enhances the sensitivity of multiple myeloma cells to bortezomib in vitro and in vivo by promoting mitochondrial pathway-mediated cell apoptosis, 2040620720932686, Therap. Adv. Hematol. 11 (2020), https://doi.org/10.1177/2040620720932686.
[29] H. Jiang, J. Xing, C. Wang, H. Zhang, L. Yue, X. Wan, W. Chen, H. Ding, Y. Xie, H. Tao, Z. Chen, H. Jiang, K. Chen, S. Chen, M. Zheng, Y. Zhang, C. Luo, Discovery of novel BET inhibitors by drug repurposing of nitroxoline and its analogues, Org. Biomol. Chem. 15 (44) (2017) 9352–9361, https://doi.org/10.1039/c7ob02369c.